Fibers and Polymers 2017, Vol.18, No.12, 2278-2286
DOI 10.1007/s12221-017-7211-y

ISSN 1229-9197 (print version)
ISSN 1875-0052 (electronic version)

Synthesis and Application of Phthalimide Disperse Dyes

Yi-zhen Zhan[1], Xue Zhao[2], and Wei Wang[1]*

[1]*College of Chem-Bio Engineering, Donghua University, Shanghai 201620, PR China*
[2]*College of Textile & Garment, Shaoxing University, Shaoxing 312000, PR China*

(Received March 5, 2017; Revised July 20, 2017; Accepted July 22, 2017)

Abstract: Three azo dyes had been synthesized using N-propyl substituted, dibromo-substituted and dicyano-substituted phthalimides as diazo components. All of the synthesized intermediates and dyes have been characterized by MS, ^{1}H-NMR and IR analyses. The dyeing behaviour and fastness properties of these dyes had been investigated. The absorption maxima of the dyes were observed in the range 360 to 700 nm. The results indicated that dyes caused hypsochromism effect after -Br substitution and dyes caused bathochromism effect after -CN substitution. IR spectra of hydrolyzed dye showed that C=O groups appeared under relatively mild alkaline conditions. Compared with electron density, steric hindrance effect is an more important influence factor than electron density in hydrolysis reaction process. Exhaustion of dyed polyester/elastane fabrics decreased obviously as the pH value increased. In order to ensure dyeing levelness, heating rate of prepared dyes will be strictly controlled. Due to alkali-clearable property and interaction energy of dye-fiber and dye-dye, the dyes have good colorfastness.

Keywords: Phthalimide, Alkali-clearable, Disperse dye, Interaction energy, Density functional theory

Introduction

Polyester fibers is usually dyed with disperse dyes. The development of polyester/elastane blends and its use in sport- and leisure-wear textile, pose washing fastness problems of disperse dyestuffs. Since the 1970s, the demand for disperse dyes that display high washing fastness on polyester is increasing. Furthermore, there are increasing global legislative pressures to reduce the impact of dyeing processes on the environment through reductions in effluent discharge [1,2].

Alkali-clearable disperse dyes offer a means of tackling both of these challenges simultaneously because the dyes can be converted to water soluble chemicals without cleavage of the azo group(s) in the dye at high temperature conditions or under relatively mild alkaline conditions [3].

The commercial alkali-clearing disperse dyes that incorporate diester or thiophene groups within the structure enabled high washing fastness have developed from 20th century, such as C.I. Disperse Red 278 and C.I. Disperse Green 9. Diester groups are hydrolyzed to the corresponding carboxylic acids, which give the dye water solubility but little or no substantivity on polyester fibers [4-6]. Thiophene groups decompose during the alkaline treatments performed on dyed fabrics to produce colorless or only slightly tinted decomposition products [7].

In recent twenty years, the others alkali-clearable dyes being investigated were based on disperse dyes containing a fluorosulfonyl group or naphthalimide group. The fluorosulfonyl group of the researching dyes is hydrolyzed by the alkali to a soluble sulfonate group [8-10]. The alkali-clearing mechanism of naphthalimide disperse dyes is the same as the diester-based disperse dye [11,12].

Koh and Kim researched the alkali hydrolysis mechanism of phthalimide-based azo disperse dyes in 1998 [13]. More recently, phthalimide-based alkali-clearable dyes have been reported [14-16]. Phthalimide-based azo disperse dyes undergo ring opening and are converted to water-soluble phthalate groups under relatively mild alkaline conditions without the breaking of azo bonds. Consequently, the hydrolyzed dye tends to be solubility during washing after dyeing and domestic laundering and remain partitioned in the liquor, lowering the degree of staining on fabrics [17].

Phthalimide disperse dyes also had better coplanar aromatic rings. One of best way to improve the washing fastness of dyes was to improve the planarity of dye molecules. Better planarity of aromatic molecules produced greater intermolecular interaction energy, lower heat migration and excellent washing fastness. To the best of our knowledge, the relationship of washing fastness and the phthalimide structure property have not been investigated. The interaction energy (such as π-π interactions) between the dyes molecule can affect dyes-dyes forces and dye-fiber forces, when benzo-heterocyclic structure was introduced into the molecular and heterocyclic structure was coplanar with the aromatic ring. But there were few relevant research reports to support this.

Here, the synthesis of N-propyl substituted (Dye-1), brominated N-propyl substituted (Dye-2) and dicyano N-propyl substituted (Dye-3) and application of phthalimide dyes to polyester fabric is detailed, investigating coloration properties in terms of hydrolyze mechanism, shade and color fastness. The synthesized intermediates and dyes were characterized by infrared spectroscopy, NMR spectroscopy and mass spectrometry. In addition, the impact of dyes structure on dyeing performance also researched with density functional theory (DFT).

*Corresponding author: wangv@dhu.edu.cn

Experimental

Materials

n-propylbromide, phthalimide, N,N-diethylaniline, copper(I) cyanide and zinc cyanide were obtained from Aladdin Industrial Corporation (China). Nitric acid, sulfuric acid, Tin(II)chloride dehydrate, hydrochloric acid, ethanol, toluene, sodium hydroxide were supplied by Xilong Chemical Co. (China), while ammonia, sodium nitrite, acetic acid, sodium acetate, bromine and triethylamine were provided by Sinopharm Chemical Reagent Co., Ltd. (China).

Synthesis of Dye Intermediates

Phthalimid intermediates and dyes were synthesized according to Scheme 1.

4-Nitrophthalimide (MA-1)

Phthalimide (80 g) was added into mixed acid which prepared from fuming nitric acid (65 %, 100 g) and concentrated sulphuric acid (98 %, 500 g) at 10 °C. The reaction mixture was then allowed to warm slowly to 25 °C. After 12 h, the reaction product was precipitated by pouring into ice (1500 g), filtered and washed with water until free from acid, and purified by recrystallisation from ethanol.

4-nitro-N-Propylphthalimide (MC-1)

MA-1 (35 g) was dissolved in DMF (300 m*l*), n-propylbromide (19 g) was added into the mixture. Triethylamine (15 g) was added slowly and stirred for 6 h at 60 °C. Following drowning onto ice, the resultant precipitate was isolated by filtration, washed with water and dried. The crude product was purified by recrystallisation from methanol.

4-Amino-N-Propylphthalimide (MC-2)

MC-1 (16.6 g) was stirred into a solution of stannous chloride dihydrate (56 g) in hydrochloric acid (37 %, 170 m*l*) and water (100 m*l*). After 2.5 h, the precipitate was collected by drowning onto ice. Filtered and washed with cold water until free from acid. The product was purified by recrystallisation from toluene.

4-Amino-3,5-dibromo-N-propylphthalimide (MC-3)

A mixture of MC-2 (10.2 g), sodium acetate (10 g) and acetic acid (150 m*l*) were stirred together at room temperature. Bromine (16 g) in acetic acid (25 m*l*) was added dropwise with thorough stirring, the reaction mixture was then drowned onto ice and the resulting product was collected by filtration, washed with water and recrystallised from ethanol.

Synthesis of Dyes

Dye-1

0.05 mol of MC-2 was diazotized in 40 m*l* of 37 % HCl and 240 m*l* of water, by adding 0.06 mol of $NaNO_2$ at a temperature of 0-5 °C. Then stirred for 5 h at 5-10 °C. The resulting solution was used immediately in the following coupling reaction. The coupling component N,N-diethylaniline (0.05 mol) was dissolved in water (200 m*l*) and hydrochloric acid (37 %, 20 m*l*) and then cooled to 0-5 °C by the addition of ice. The diazonium solution previously prepared was added dropwise over 30 min at the same temperature. The mixture was stirred for a further 5 h at 5-10 °C and then

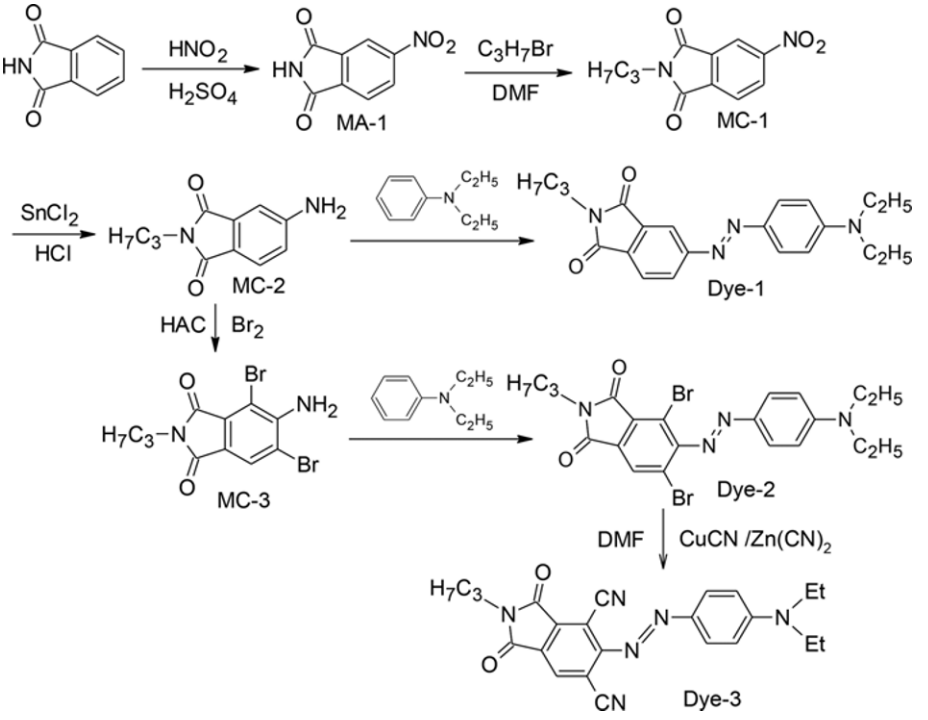

Scheme 1. Synthesis of compounds dyes.

aqueous sodium hydroxide solution (10 %) was added slowly below 10 °C until the pH rose to within the range of 3-4. The precipitated product was filtered off, washed with water until the filtrate was pH 6-7 and dried. The crude dyes were purified by recrystallisation from ethanol.

Dye-2 was prepared using the same procedure as the preparation of Dye-1.

Dye-3

A mixture of Dye-2 (0.05 mol), zinc cyanide (0.055 mol) and copper(I) cyanide (0.025 mol) in DMF (125 m*l*) was stirred at 90 °C. After 3 h, the reaction mixture was added onto ice to precipitate the product, which was then filtered off, washed with water and dried at 70-75 °C. The crude dyes were purified by recrystallisation from ethanol.

Dye Application

Dyeing was carried out with a laboratory dyeing machine (Yabo, China). 5.0 g polyester/spandex blends fabric (95:5) was dyed at 130 °C×50 min with a liquor ratio of 15:1. The dye concentration was 2 % (o.w.f) and the dyebath was adjusted to pH 4.5 using acetic acid/sodium acetate. For the dyeing rate curve, the dyeing process was interrupted at different temperatures during the heating stage (80 °C, 90 °C, 100 °C, 110 °C, 120 °C and 130 °C) and at different times during the isothermal step at 130 °C (10 min, 20 min, 30 min, 40 min and 50 min). For the dyeing pH value, different pH values (pH=3.0, 5.0, 7.0, 9.0, 11.0) were chosen. Both of the dyes were applied at 2 % (o.w.f) to the fabric samples for evaluating the washing and perspiration fastness.

After dyeing, the samples were washed with warm water of 50 °C and then clearing at 80 °C for 15 min (2 g/*l* NaOH). The reduction cleared samples were rinsed with water and dried at 190 °C×40 s.

Alkali Solubility of Synthesized Dyes

0.02 g synthesized dyes dissolved in 1 g/*l* NaOH solution at 40 °C, 60 °C, 80 °C respectively, absorption spectra from 360 nm to 700 nm were measured with spectrophotometer.

Characterization

pH Value

pH value was measured using ray magnetic PHS-25 pH meter (Jing Branch, China).

Colorimetric Evaluation

K/S value and color depth of disperse dyes on polyester/spandex blends fabric is obtained from dyed sample at the maximum wavelength by using a spectrophotometer Datacolor SF 600 PLUS-CT (Datacolor, USA). Color measurement conditions: CIE standard illuminant D_{65}, 10 ° observer, ultraviolet included, specular component included, large aperture. The samples were measured at four readings rotated 90 ° and the color intensity results averaged.

The colour strength (*K/S*) was calculated on the basis of the Kubelka-Munk equation (1):

$$K/S = \frac{(1-R)^2}{2R} \quad (1)$$

where *K* is the adsorption coefficient, *R* is the reflectance of the dyed sample, and *S* is the scattering coefficient.

Color depth was calculated using equation (2):

$$\text{Color-depth} = \int_{380nm}^{700nm} f(x)_{k/s} dx \quad (2)$$

where $f(x)$ is the integral function of *K/S* curve from 380 nm to 700 nm.

Color intensity is the ratio of color-depth$_{\text{batch-sample}}$ and color-depth$_{\text{standard-sample}}$, which was obtained from the spectrophotometer directly, as shown in equation (3).

$$\text{Color intensity (\%)} = \frac{\text{Color-depth}_{\text{batch-sample}}}{\text{Color-depth}_{\text{standard-sample}}} \times 100\% \quad (3)$$

Spectrophotometry

^{1}H-NMR spectra were obtained using an Bruker Advance Digital 400 (Swistzerland) at 400 MHz for solutions in solvent $CDCl_3$. Mass spectrometry (MS) was carried out using a Shimadzu GCMS-QP2010Ultra spectrometer (Japan). The absorption spectra were measured on an Tianmei 8500 UV-VIS spectrophotometer (China). A Nicolet 6700 (Thermo Fisher, USA) equipped with an attenuated total internal reflectance (ATR) accessory was used to analyse chemical functionalities of samples.

Determination of Dye Exhaustion Yields

Dye uptake was determined by measuring absorbance of diluted dyebath samples at the wavelength of the maximum absorption (λ_{max}) of the dye. The percentage of dye bath exhaustion (%E) was calculated using equation (4):

$$\%E = \frac{A_0 - A_1}{A_0} \times 100 \quad (4)$$

where A_0 and A_1 are the absorbances at λ_{max} of the diluted dyebath samples obtained prior to dyeing and after dyeing, respectively.

Wash Fastness Test

The color fastness to washing was determined in accordance with the ISO 105-C06: 2010 (B1S) using rotawash washing machine (SDL-Atlas, USA). The color fastness to perspiration and dye transfer was determined in accordance with the ISO 105-E04: 2013 and AATCC 163: 2013 using Binder oven (Binder, Germany). The degree of color staining on the multifiber were assessed using Datacolor SF 600 PLUS-CT (USA).

Density Functional Theory Calculations

Geometry optimization calculation and the stable ground state configuration and unit cell parameter of synthesized dyes were obtained using the DFT/B3LYP method, combined with the 6-311G (d) basis set. Homo and LUMO molecular orbital and energy were obtained using the DFT/B3LYP method, combined with the 6-311G++(d,p) basis set.

Molecular ring interaction energy studied using density functional ωB97XD function, basis set selection 6-311G++ (d,p).

Results and Discussion

Infrared Spectra Analysis

The FTIR spectra of intermediates and dyes recorded in the range of 500-4000 cm^{-1} are presented in Figure 1. FTIR spectrum of MA-1 shows a broad absorption band centered at 3319 cm^{-1} is attributed to stretching vibrations of -NH- of phthalimide group. The two absorption bands near 1731 cm^{-1} and 1698 cm^{-1} are identified as C=O stretching vibration. The FTIR spectrum of intermediates and dyes also shows a number of characteristic absorption bands. The peak at 1542 cm^{-1}, 1346 cm^{-1} is associated with the stretching vibrations of $-NO_2$. The lower peak at 2959 cm^{-1} and 2875 cm^{-1} were the contribution of $-CH_3$, $-CH_2$ stretching vibration from propyl group. The main peaks appear at 3479 cm^{-1} and 3372 cm^{-1} of MC-2 and MC-3 are related with the formation of $-NH_2$ group. The peaks located at 1535 cm^{-1} of Dye-1 and Dye-2 are attributed to stretching vibration of -N=N-. The peak appeared at 2225 cm^{-1} is associated with the stretching vibrations of -CN.

Mass and ^{1}H-NMR Analysis

Mass and ^{1}H-NMR spectroscopy data of intermediates and dyes are as follows. The mass analysis results are consistent with the theoretical molecular weight and this data support that the intermediates and dyes are synthesized properly.

MA-1: MS, m/z: 192. ^{1}H-NMR ($CDCl_3$): δ=8.08-8.10 (1H, d, Ar-H), 8.64-8.71 (2H, t, Ar-H), 11.77 (1H, s, -NH) ppm.

MC-1: MS, m/z:234. ^{1}H-NMR ($CDCl_3$): δ=0.93 (3H, t, $-CH_3$), 1.58-1.68 (2H, m, $-CH_2$), 3.72 (2H, t, N-CH_2), 8.04-8.68 (3H, m, Ar-H)ppm.

MC-2: MS, m/z: 204. ^{1}H-NMR ($CDCl_3$): δ=0.93 (3H, t, $-CH_3$), 1.68-1.70 (2H, m, $-CH_2$), 3.60 (2H, t, N-CH_2), 6.47 (2H, s,$-NH_2$), 6.82-7.63 (3H, m, Ar-H)ppm.

MC-3: MS, m/z: 362. ^{1}H-NMR ($CDCl_3$): δ=0.91 (3H, t, $-CH_3$), 1.64 (2H, m, $-CH_2$), 3.57 (2H, m, N-CH_2), 6.36 (2H, s, $-NH_2$), 7.84 (H, d, Ar-H)ppm.

Dye-1: MS, m/z: 364. ^{1}H-NMR ($CDCl_3$): δ=0.9-1.1 (3H, m, $-CH_3$), 1.2-1.5 (6H, m, $-CH_3$), 1.60-1.80 (2H, m, $-CH_2$), 3.60 (2H, t, N-CH_2), 6.80 (2H, m, Ar-H), 7.81-8.73 (5H, m, Ar-H)ppm.

Dye-2: MS, m/z: 522. ^{1}H-NMR ($CDCl_3$): δ=0.93 (3H, t, $-CH_3$), 1.16 (6H, t, 2×CH_3), 1.60 (2H, m, $-CH_2$), 3.40 (4H, q, 2×CH_2), 4.33 (2H, t, N-CH_2), 6.91 (2H, d, Ar-H), 8.05 (2H, d, Ar-H), 8.20 (H, s, Ar-H)ppm.

Dye-3: MS, m/z: 414. ^{1}H-NMR ($CDCl_3$): δ=0.96 (3H, t, CH_3), 1.25 (6H, t, 2×CH_3), 1.68 (2H, m, CH_2), 3.68 (4H, q, 2×CH_2), 3.88 (2H, t, N-CH_2), 6.88 (2H, d, Ar-H), 8.00 (H, d, Ar-H), 8.30 (H, s, Ar-H) ppm.

Dyes Color Shade

The maximum absorption wavelength (λ_{max}) of Dye-1, Dye-2 and Dye-3 were shown in Figure 2, λ_{max} of Dye-1, Dye-2 and Dye-3 were 496 nm, 440 nm and 565 nm respectively. Dye-1 was red shade color, Dye-2 was yellow shade color and Dye-3 was purple shade color, which indicated that Dye-2 caused hypsochromism effect after -Br substitution and Dye-3 caused bathochromism effect after -CN substitution. Figure 3 showed that the substitution of -Br damaged the molecular planarity structure and the conjugate system. For example, the dihedral angle between the phthalimide ring and the benzene ring of Dye-1, Dye-2 and Dye-3 were 2.27 °, 50.84 ° and 1.99 °. The 50.84 ° distortion angle of phthalimide structure and a benzene ring mainly because of the steric hindrance effects between two ortho-substituted dibromo atoms at positions of the phthalimide phenyl ring and the azo unit. Introduction of dibromo atoms

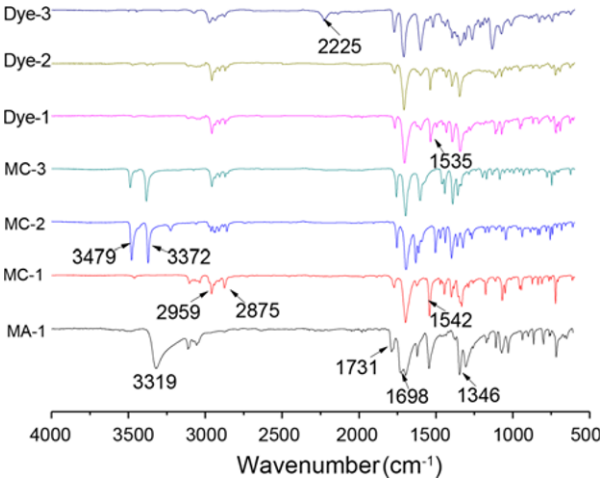

Figure 1. IR spectrum of intermediates and dyes.

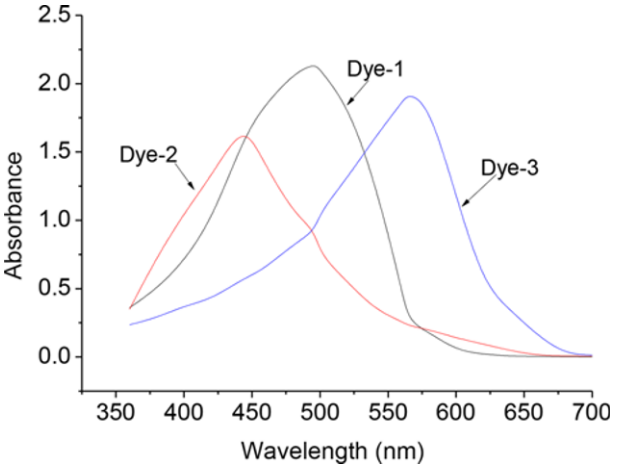

Figure 2. Absorbance curve of dyes.

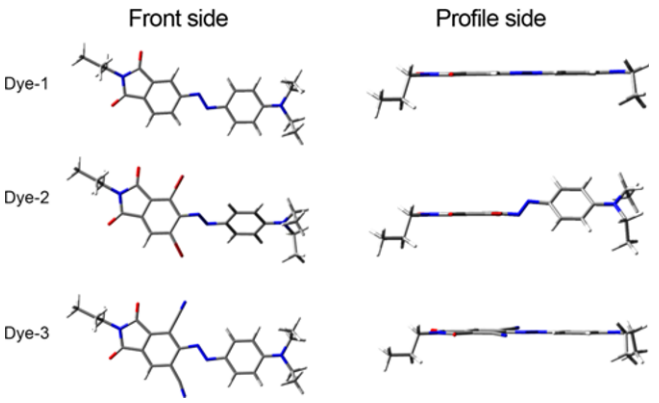

Figure 3. Optimized phthalimide structure.

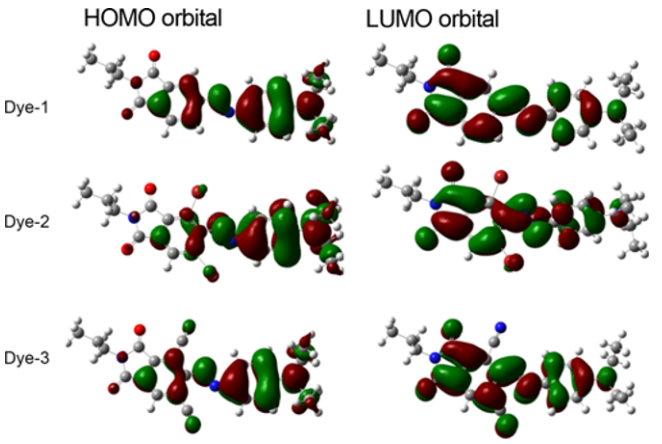

Figure 4. Dyes HOMO and LUMO orbital.

hindered electron transfer and increased the stimulate transition energy.

According to quantum theory, the dye shade happens because electronic transitions between the ground state and the excited state, and the electronic transitions needs stimulate transition energy ΔE (energy between ground state and excited state), $\Delta E=h\nu=hc/\lambda_{max}$, that's to say the greater the ΔE, the further λ_{max} will be shifted towards shorter wavelength (hypsochromism). The smaller the ΔE, the further λ_{max} will toward longer wavelength (bathochromism). In general, $\Delta E_{HOMO\rightarrow LUMO}$ (ground state→first excited state) between the highest occupied molecular orbital (HOMO) and lowest unoccupied molecular orbital (LUMO) is the smallest one in stimulate transition energy ΔE, the corresponding wavelength is in the visible range, so the $\Delta E_{HOMO\rightarrow LUMO}$ is an important parameter.

The substituents on the diazo phthalimide components will inflence the differences of ΔE and λ_{max}. According DFT energy calculation results in Table 1, $\Delta E_{HOMO\rightarrow LUMO}$ of Dye-1, Dye-2 and Dye-3 were 2.857 eV, 3.035 eV and 2.561 eV, respectively. -Br substitution in Dye-2 lead to significant twisting about the linkage between the azo bridge and the diazo component ring, reducing orbital overlap, which in turn resulted in an increase in transition energies and a hypsochromic shift, the hypsochromic shifts ($\Delta\lambda_{max\ Cal.}$ is 18 nm and $\Delta\lambda_{max\ Exp.}$ is 47 nm) in the dibromo dyes-2 when compared with their non-brominated analogues Dye-1. -CN is a rod-like shape, steric hindrance is relatively insignificant while electron withdrawal (through resonance and induction) by the group dominates, lowering ΔE, manifested by bathochromism. This effect is also seen when comparing dyes-1 and dyes-3 where the bathochromic shift $\Delta\lambda_{max\ Exp.}$ is 78 nm. The changing trends of $\lambda_{max\ Cal.}$ and $\lambda_{max\ Exp.}$ were similar in the comparisons, confirming the accuracy of the results.

Table 1. Substituent effects on λ_{max}

	E_{HOMO} (eV)	E_{LUMO} (eV)	$\Delta E_{HOMO\rightarrow LUMO}$ (eV)	$\lambda_{max\ Cal.}$ (nm)	$\lambda_{max\ Exp.}$ (nm)
Dye-1	-5.697	-2.840	2.857	463	487
Dye-2	-5.834	-2.799	3.035	445	440
Dye-3	-6.077	-3.516	2.561	513	565

The difference $\Delta E_{HOMO\rightarrow LUMO}$ of Dye-1, Dye-2 and Dye-3 could be seen from the HOMO and LUMO orbit diagram, as shown in Figure 4. Propyl was not involved in the molecular conjugate structure and had little impact on electron cloud distribution. HOMO and LUMO orbit electron cloud distribution was relatively concentrated due to the substitution of Br-. Electronic transitions between HOMO and LUMO was more difficulty because of un-planarity, which caused the higher $\Delta E_{HOMO\rightarrow LUMO}$ of Dye-2. Compared with Dye-1, HOMO and LUMO orbital electron distribution of Dye-3 did not change obviously and the rod-shaped -CN group was also involved in frontier orbitals of conjugated system, which caused electron dispersion and migration in the molecule more effortlessly, resulted in bathochromism.

Dye Structure and Dyeing pH Value

Figure 5 showed the influence of pH value on exhaustion, exhaustion decreased obviously as the pH value increased. For example, Dye-1, Dye-2 and Dye-3 exhaust less (24 %, 15 % and 24 % respectively) at pH=9 than that of at pH=3 (84 %, 61 % and 77 % respectively). Meanwhile exhaustion at pH=11 of Dye-1, Dye-2 and Dye-3 were 17 %, 10 % and 12 % respectively. The synthesized dyes hydrolyzed with pH value increased at high temperature.

Figure 6 was IR spectra of hydrolyzed dye. Compared with the unsubstituted dye (UDye), the peak at 1770 cm^{-1} and 1395 cm^{-1} of hydrolyzed dye (HDye) were the contribution of C=O stretching vibration from carboxylic acid group, which indicated that the phthalimide ring in the structure of these synthesized dyes undergoes ring opening, amide groups converts to a water-soluble carboxylic acid groups by hydrolysis under relatively mild alkaline conditions. Carboxylate salt group increased the dye water-solubility and reduced the

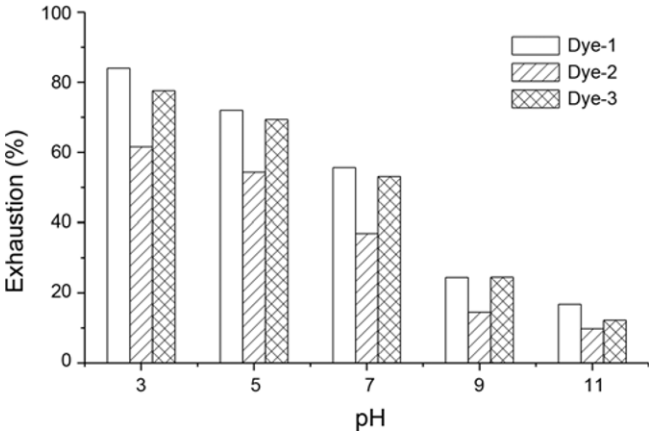

Figure 5. Influence of pH value to exhaustion.

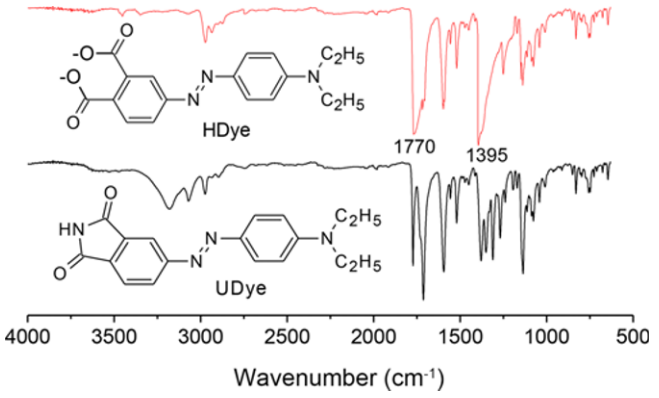

Figure 6. Hydrolyzed dye IR spectrum.

fiber-dye affinity.

Dye Structure and Alkali Solubility

Figure 7 showed the absorption spectra of Dye-1, Dye-2 and Dye-3 dissolved in alkali solution at temperature 40 °C, 60 °C and 80 °C. Different from reduction clearing in which azo link of the dye was broken by the action of the reducing agent and the dye became colorless. Since the azo link of the dye was not broken and the dyes π-conjugated system was not destroyed by the action of the alkali agent. In the case of alkali dissolving, the production of arboxylate salt group increased the dye water-solubility at higher temperature and the absorption spectrum shows a tendency for gradual increase of the absorbance at λ_{max}. These results implied that the amount of water-soluble phthalate salt increased due to hydrolysis of dye at higher temperature.

According to Scheme 2, the dye hydrolysis mechanism is that the nucleophile OH^- attacks the carbon with an electropositive (10C and 12C), breaking the C-N group bond and forming the C-O bond through a transition state.

One of hydrolysis influence factor is the electron density distribution on 10C, 41N and 12C, the more positive charge on 10C and 12C, the more attack will be happened on dyes,

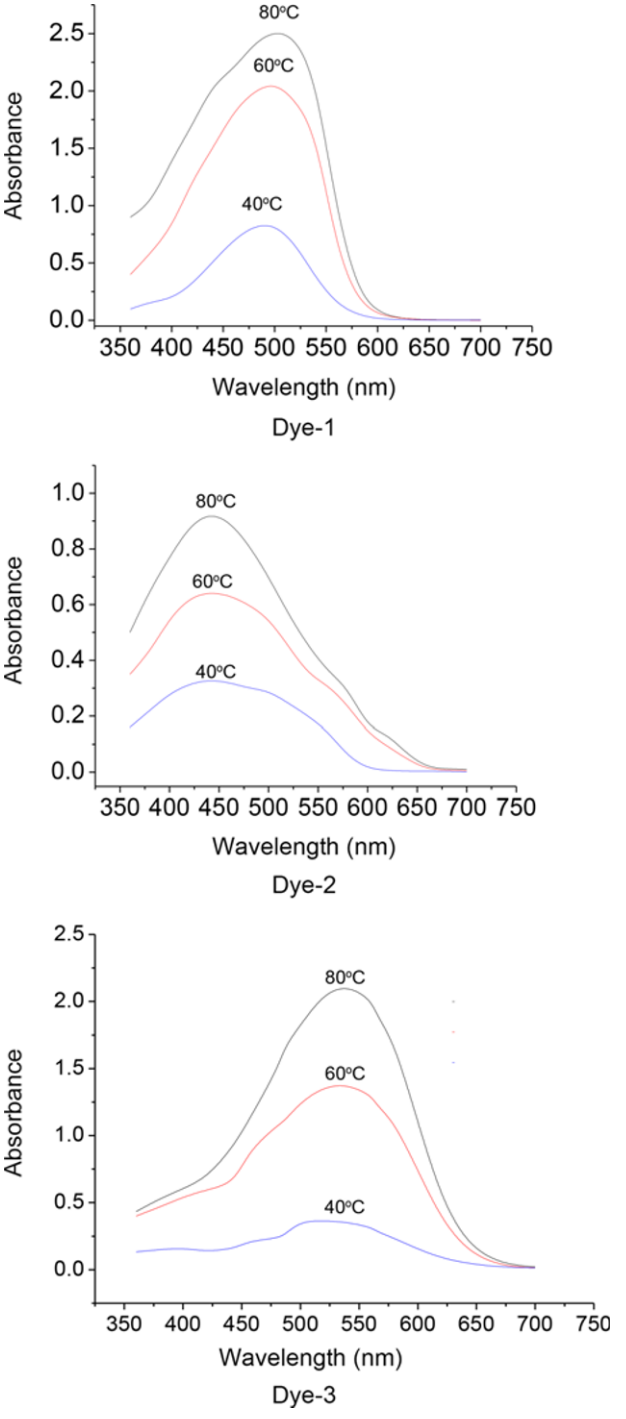

Figure 7. Alkali solubility curve at different temperature.

and dyes will be more easily hydrolyzed. The other hydrolysis influence factor is steric hindrance effect. Because substituted groups on phthalimide moiety will hinder the approach of OH^- to the 10C and 12C. So hydrolysis reaction will increase with higher positive charge of 10C and 12C and little substituted group steric hindrance.

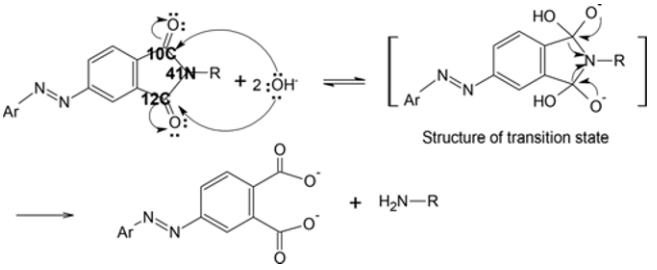

Scheme 2. Hydrolysis mechanism of dyes.

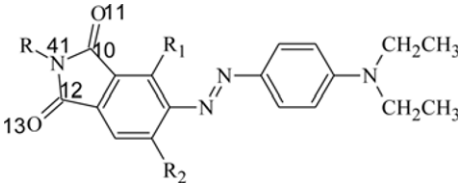

Table 2 showed that, compared with the Dye-1, positive charge on 10C and 12C enhanced after Br- and CN-substitution. This described that Dye-2 and Dye-3 would be hydrolyzed more easily to converse to water-soluble products compared with Dye-1 during the high-temperature dyeing process, alkaline wash-off process and so on.

Contrast to the electron density results, however, Figure 8 showed the opposite results. The color intensity of the synthesized dyes at pH=3 is 100 %, the color intensity of pH=7 and pH=11 of Dye-1 is the lowest. The variations in the different substituent dyes (Dye-1, Dye-2 and Dye-3) also can be seen from the Figure 8, the color intensity of pH=7 and pH=11 of Dye-2 was the highest which meant Dye-2 was more difficulty to be hydrolyzed. According to Gabriel reaction, hydrolysis reaction of phthalimide disperse dye is nucleophilic addition-elimination reaction. The results in Figure 8 indicated that the steric hindrance effect is an more important influence factor than electron density in hydrolysis reaction process. Bromo and cyano functions increased the hindrance while decreased the hydrolysis, the color intensity of pH=7 and pH=11 of Dye-2 and Dye-3 is higher than that of Dye-1. And the rod-like shape and the higher electron density of cyano are responsible for easier hydrolysis of Dye-3 when compared with the bromo analogues Dye-2.

Table 2. Electron cloud density of 10C, 41N, 12C

	10C	41N	12C
Dye-1	0.5785	-0.5504	0.5754
Dye-2	0.6018	-0.5530	0.5801
Dye-3	0.6062	-0.5555	0.5845

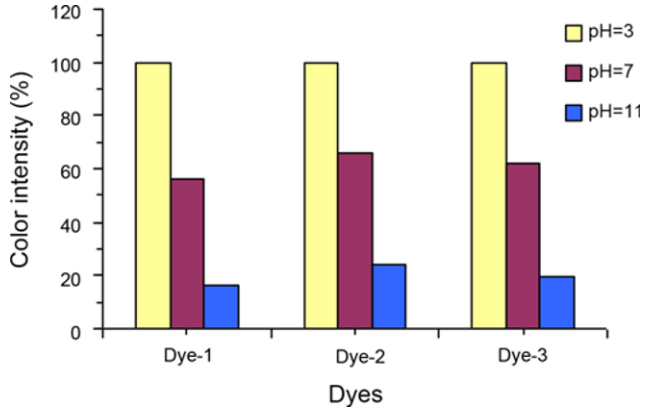

Figure 8. Influence of pH value on color intensity.

Dyeing Rate Curve

Reasonable dyeing process would be set up according to dyeing curve. Figure 9 showed that dyeing rate of synthesized dyes at temperature 80 °C-130 °C was slower than S-type dyeing disperse dyes (C.I. Disperse Red 167, C.I. Disperse Orange 30 and C.I. Disperse Blue 79). Dye-1, Dye-2 and Dye-3 could not achieve maximum uptake until 130 °C× 10 min and reach dyeing equilibrium until 130 °C×20 min. Different from equilibrium dyeing temperature at 110-130 °C of S-type dyeing disperse dyes, the dyeing temperature of Dye-1, Dye-2 and Dye-3 may be 135 °C in order to ensure dyeing levelness, and heating rate will be strictly controlled.

The results showed that there was larger dye interaction energy in synthesized dyes than S-type dyeing disperse dyes. Disperse dyeing of polyester fibers follows a solid-solid interaction where a solid dye is solubilised in another solid fiber phase. The disperse dyes in solid form or in micelle form dissolved into single dye molecule in water and dyed on the fibers. Slow dyeing rate means more energy was needed to damage dye-dye interaction energy. Phthalimide group has better coplanarity. Meanwhile phthalimide group contains electron-rich hetero-atoms N, O and electron-deficient phenyl ring, which will generated electrostatic potential energy and affect the dye-dye, dye-fiber interaction. The slow adsorption rate exerted by phthalimidyl azo dyes could be found the same phenomenon as benzodifuranone-based disperse dyes in a previous study [18].

Polyester fiber molecular is polyethylene terephthalate;

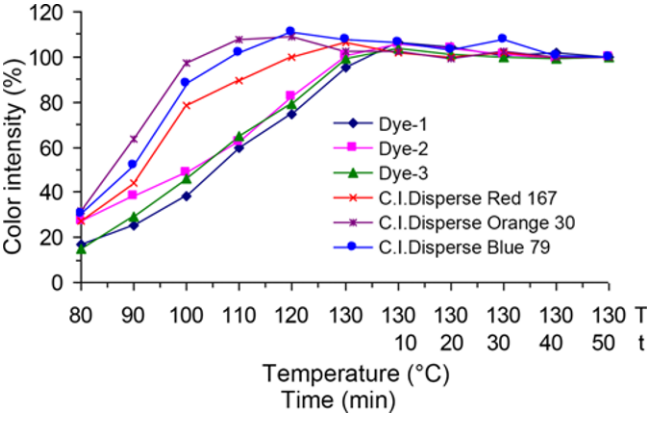

Figure 9. Dyes time-temperature curve.

most of disperse dyes applied on polyester fiber are single azo structure, both of polyester and the single azo disperse dye molecules contain a single aromatic benzene ring structure, the inter aromatic-rings forces is benzene-benzene interaction energy. Phthalimide disperse dyes contain phthalimide group, the aggregated dye-dye inter aromatic-rings forces is phthalimide-phthalimide interaction energy, the dye-fiber inter aromatic-rings forces is phthalimide-benzene interaction energy. The interaction energy of disperse dyes in polyester amorphous regions mainly including π-π stacking interaction and van der Waals of aromatic-aromatic

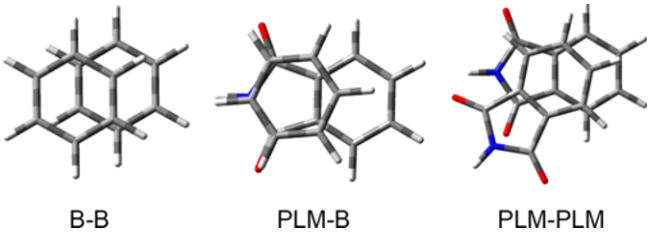

Figure 10. Optimized dimer configuration.

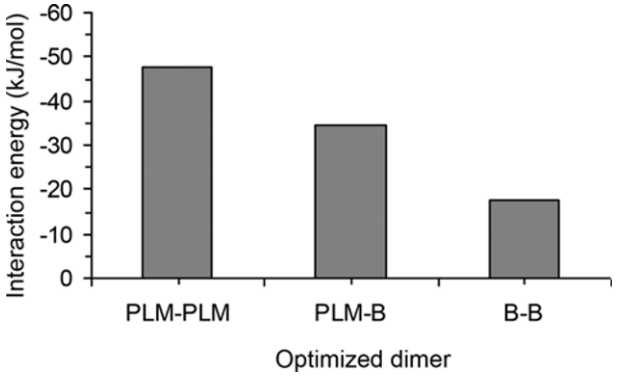

Figure 11. Optimized dimer interaction energy.

force between polyester molecules and disperse dyes. The larger interaction energy between disperse dyes-disperse dyes, disperse dyes-fibers, the harder will the dye molecules migrate to the fiber surface under the external conditions such as high temperature and solvent effects, thereby improving the wash fastness property.

In order to investigate the influence of phthalimide in aromatic rings interaction energy, benzene and phthalimide group optimized at ωB97XD/6-311G (d, p) level firstly, then optimized benzene-benzene (B-B), phthalimide-benzene (PLM-B) and phthalimide-phthalimide (PLM-PLM) dimers were set up with optimized configuration, optimized interaction energy shown in Figure 10 and Figure 11.

Figure 11 showed that optimized phthalimide-phthalimide, phthalimide-benzene and benzene-benzene dimer interaction energy were -47.78 kJ/mol, -34.66 kJ/mol and -17.59 kJ/mol, respectively. Phthalimide-phthalimide and phthalimide-benzene interaction energy were much larger than that of benzene-benzene. As for disperse dyes, preferably coplanarity phthalimide structure can improve interaction energy between the dye-dye and the dye-fiber. That's also to say phthalimide disperse dyes are more difficult to migrate to the surface which improves the dye color fastness to washing.

Colorfastness

Usually, the nylon, diacetate, polyester and wool components of multifiber adjacent fabrics are particularly prone to staining while acrylic and cotton suffered less staining during colorfastness testing of disperse-dyed polyester fabrics.

Fastness values for the staining of these multifibers are presented in Table 3. The synthesized phthalimide-base dyes showed excellent levels of colorfastness to washing, perspiration and dye transfer. The tested samples only were washed with 2 g/*l* NaOH and dried at 190 °C×40 s. Alkali washed fabrics exhibited high washing and perspiration fastness, presumably

Table 3. Colorfastness of synthesized dyes

			Wool	Acrylic	Polyester	Nylon	Cotton	Diacetate
Dye-1	WI		4	5	3-4	3-4	5	3-4
	PI	Acid	5	5	5	4	5	4
		Alkali	5	5	5	4	5	4
	DT		5	5	5	4-5	5	4-5
Dye-2	WI		5	5	4-5	4	5	4
	PI	Acid	5	5	5	4-5	5	4-5
		Alkali	5	5	5	4-5	5	4-5
	DT		5	5	5	5	5	5
Dye-3	WI		5	5	4-5	4	5	4-5
	PI	Acid	5	5	5	4-5	5	4-5
		Alkali	5	5	5	4-5	5	4-5
	DT		5	5	5	5	5	5

WI: washing fastness, PI: perspiration fastness, DT: dye transfer fastness.

because the phthalimide ring of the dyes is hydrolyzed to solubilising groups. These hydrolyzed dyes are readily removed by alkaline wash-offs and exhibit good wet fastness.

In addition, the good dye transfer fastness might be explained by interaction energy between the dye-dye and the dye-fiber, which instructed that a bigger energy was needed to destroy the dye-fiber and dye-dye interaction energy.

Conclusion

N-propyl substituted, dibromo-substituted and dicyano-substituted phthalimides dispese dyes were synthesized through nitration, alkylation, amination, bromination, diazotization coupling reaction. All of the synthesized intermediates and dyes have been characterized by MS, ^{1}H-NMR and IR analyses.

The gamut of colour of the two dyes spanned much of the visible spectrum: absorption maxima of the dyes in formamide were observed in the range 360 to 700 nm. N-propyl substituted dye is red shade color while dibromo-substituted is yellow shade color, which indicated that Dye-2 caused hypsochromism effect after -Br substitution and Dye-3 caused hypsochromism effect after -CN substitution. The dihedral angle, $\Delta E_{HOMO \rightarrow LUMO}$ and HOMO and LUMO orbit diagram of DFT calculation results proved the experimental result.

In the case of alkali dissolving, the absorbance at λ_{max} tends to increased with increase temperature. This result implies that the amount of water-soluble phthalate salt increases due to hydrolysis of dye. The peak at 1770 and 1395 cm^{-1} in IR spectra of hydrolyzed dye showed that C=O groups appeared under relatively mild alkaline conditions. Hydrolysis influence factor are electron density distribution and steric hindrance effect. Compared with electron density, steric hindrance effect is an more important influence factor than electron density in hydrolysis reaction process. Exhaustion of dyed polyester/elastane fabrics decreased obviously as the pH value increased.

Dyeing rate of prepared dyes at temperature 80-130 °C was slower than S-type dyeing disperse dyes (C.I. Disperse Red 167, C.I. Disperse Orange 30 and C.I. Disperse Blue 79). In order to ensure dyeing levelness, heating rate of prepared dyes will be strictly controlled. Phthalimide-phthalimide and phthalimide-benzene interaction energy were much larger than that of benzene-benzene. Due to alkali-clearable property and interaction energy of dye-fiber and dye-dye, the dyes have good colorfastness.

References

1. J. Koh, H. Kim, J. Lee, and M. Eom, *Color. Technol.,* **125**, 322 (2009).
2. J. H. Choi, J. S. Park, M. H. Kim, H. Y. Lee, and A. D. Towns, *Color. Technol.,* **123**, 379 (2007).
3. J. H. Choi, J. Y. Choi, E. M. Kim, J. P. Kim, A. D. Towns, and C. Yoon, *Color. Technol.,* **129**, 352 (2013).
4. Z. H. Cui, X. H. Cheng, X. Li, H. H. Lu, X. D. Wang, and W. G. Chen, *Chinese Chem. Lett.*, **25**, 1121 (2014).
5. J. H. Choi, H. Y. Lee, and A. D. Towns, *Fiber. Polym.*, **11**, 199 (2010).
6. J. H. Choi and A. D. Towns, *Color. Technol*., **117**, 127 (2001).
7. G. Hallas and A. D. Towns, *Dyes Pigment*., **32**, 135 (1996).
8. J. S. Koh and J. S. Park, *Fiber. Polym.*, **9**, 128 (2008).
9. J. S. Koh and D. H. Cho, *Fiber. Polym.*, **5**, 134 (2004).
10. J. Koh, H. Kim, and J. Park, *Fiber. Polym*., **9**, 143 (2008).
11. K. Gharanjig, M. Arami, H. Bahrami, B. Movassagh, N. M. Mahmoodi, and S. Rouhani, *Dyes Pigment*., **76**, 684 (2008).
12. M. S. Kiakhani, M. Arami, K. Gharanjig, J. Mokhtari, and N. M. Mahmoodi, *Fiber. Polym*., **10**, 446 (2009).
13. J. S. Koh and J. P. Kim, *Dyes Pigment.*, **37**, 265 (1998).
14. J. H. Choi, J. M. Jeon, M. H. Kim, A. D. Towns, and C. Yoon, *Color. Technol.,* **124**, 92 (2008).
15. J. H. Choi, J. Y. Choi, H. Y. Lee, A. D. Towns, and C. Yoon, *Color. Technol*., **124**, 364 (2008).
16. J. H. Choi, O. T. Kwon, H. Y. Lee, A. D. Towns, and C. Yoon, *Color. Technol*., **126**, 237 (2010).
17. C. Matthew, "Handbook of Textile and Industrial Dyeing", 2nd ed., pp.367-370, Woodhead Publishing Ltd., Cambridge, UK, 2011.
18. Y. Z. Zhan, X. Zhao, and W. Wang, *Color. Technol*., **133**, 50 (2017).